Cell, Vol. 86, 811–822, September 6, 1996, Copyright ©1996 by Cell Press

Xeroderma Pigmentosum Group F Caused by a Defect in a Structure-Specific DNA Repair Endonuclease

Anneke M. Sijbers,*§ Wouter L. de Laat,*§ Rafael R. Ariza,†§ Maureen Biggerstaff,†§ Ying-Fei Wei,‡ Jonathan G. Moggs,† Kenneth C. Carter,‡ Brenda K. Shell,‡ Elizabeth Evans,† Mariska C. de Jong,* Suzanne Rademakers,* Johan de Rooij,* Nicolaas G. J. Jaspers,* Jan H. J. Hoeijmakers,* and Richard D. Wood†

*Department of Cell Biology and Genetics
Medical Genetics Centre
Erasmus University
3000 DR Rotterdam
The Netherlands

†Imperial Cancer Research Fund
Clare Hall Laboratories
South Mimms, Herts EN6 3LD
United Kingdom

‡Human Genome Sciences, Inc.
9410 Key West Avenue
Rockville, Maryland 20850

Summary

Nucleotide excision repair, which is defective in xeroderma pigmentosum (XP), involves incision of a DNA strand on each side of a lesion. We isolated a human gene homologous to yeast *Rad1* and found that it corrects the repair defects of XP group F as well as rodent groups 4 and 11. Causative mutations and strongly reduced levels of encoded protein were identified in XP-F patients. The XPF protein was purified from mammalian cells in a tight complex with ERCC1. This complex is a structure-specific endonuclease responsible for the 5′ incision during repair. These results demonstrate that the *XPF*, *ERCC4*, and *ERCC11* genes are equivalent, complete the isolation of the XP genes that form the core nucleotide excision repair system, and solve the catalytic function of the XPF-containing complex.

Introduction

A coordinated interplay between multiple subunits is required to carry out nucleotide excision repair (NER) in eukaryotes. The first steps of the process lead to lesion recognition and incision of the damaged strand on each side of a lesion. A 24–32 mer oligonucleotide is removed, followed by gap-filling DNA synthesis (Friedberg et al., 1995; Huang et al., 1992; Moggs et al., 1996). In human cells, this repair pathway involves the xeroderma pigmentosum (XP) proteins and associated factors. Individuals with XP show hypersensitivity to sunlight and a greatly increased incidence of skin cancer. Genes encoding the XPA, XPB, XPC, XPD, and XPG proteins have been isolated (Hoeijmakers, 1994), and a factor defective in at least some XPE cells has also been identified, although it is not required for the core NER system (reviewed by Wood, 1996). XP-F is the only remaining NER–defective XP group for which a complementing cDNA has yet to be identified.

There is evidence that the two incisions made during NER are catalyzed by separate DNA endonucleases. In humans, XPG endonuclease makes the 3′ incision relative to the lesion (O'Donovan et al., 1994a; Matsunaga et al., 1995). XPG and its yeast homolog Rad2 specifically cleave near junctions of unpaired and duplex DNA, cutting the strand in which the unpaired region moves from 3′ to 5′ away from the junction (O'Donovan et al., 1994a; Harrington and Lieber, 1994; Habraken et al., 1995). In Saccharomyces cerevisiae, the Rad1 and Rad10 proteins form a heterodimeric complex having a structure-specific endonuclease activity with a polarity opposite to XPG and Rad2, leading to the assumption that the Rad1–Rad10 complex makes the 5′ incision during NER in yeast (Bardwell et al., 1994; Davies et al., 1995). ERCC1 is the mammalian homolog of Rad10 (van Duin et al., 1986) and has been found to associate with activities that correct human XP-F cell extracts as well as extracts from Chinese hamster cells of repair complementation groups 4 and 11 (Biggerstaff et al., 1993; van Vuuren et al., 1993). A polypeptide of relative molecular mass of approximately 115 kDa has been observed to copurify with ERCC1 by several assays and has been proposed as a candidate for a Rad1 homolog (van Vuuren et al., 1995; Aboussekhra et al., 1995; Park et al., 1995). We decided to search directly for a human homolog of S. cerevisiae Rad1 and test it for possible correcting activity in XP-F and rodent group 4 and 11 cells and extracts.

Results

Isolation of a Human Homolog of Yeast Rad1

A pair of approaches were combined to isolate a human homolog of Rad1. Degenerate primers designed on the basis of homology between S. cerevisiae Rad1 (Reynolds et al., 1987), Schizosaccharomyces pombe rad16 (Carr et al., 1994), and Drosophila melanogaster MEI-9 (Sekelsky et al., 1995) were used in a reverse transcriptase–polymerase chain reaction (RT–PCR). The amplified sequence was used as a probe to isolate a human cDNA clone coding for an open reading frame with sequence similarity to the C-terminal half of Rad1 and its homologs. The N-terminal half of the human gene was identified in a database search using S. cerevisiae Rad1 and S. pombe rad16, which detected two human expressed sequence tag clones encoding an open reading frame that overlapped with the RT–PCR clone. RACE (rapid amplification of cDNA ends)–PCR confirmed the expressed sequence tag sequence. The compiled sequence of the assembled cDNA (shown schematically in Figure 1a) contains an open reading frame that encodes 905 amino acids (EMBL accession number U64315 for nucleotide sequence). The sequence context of the first ATG in the clone at position 16 matches the

§ These authors contributed equally to this work.

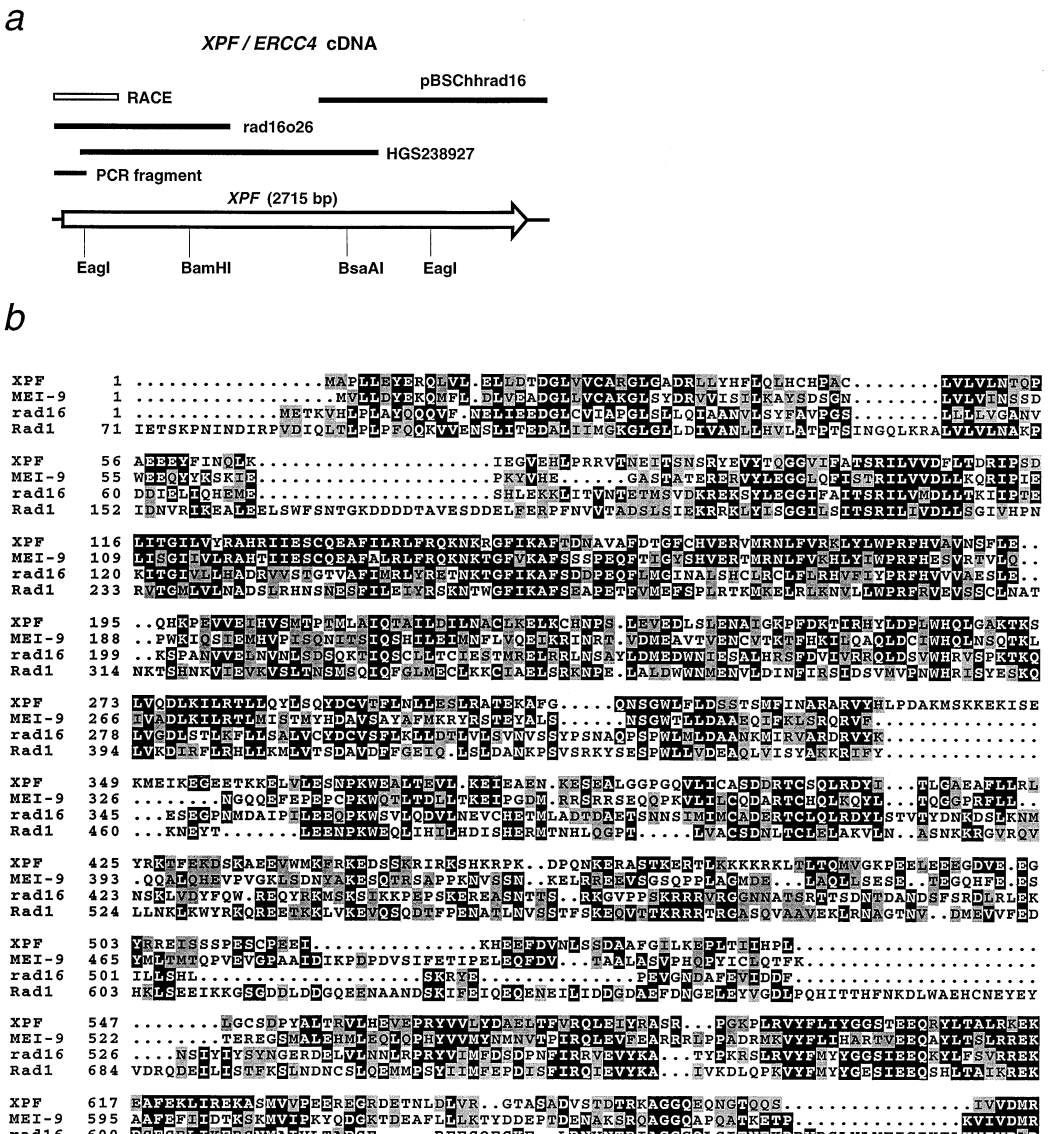

Figure 1. Cloning of a Human *RAD1* Homolog

(a) Schematic representation of the sources of cDNA used to assemble the functional gene. The open reading frame is indicated by an arrow. (b) Alignment of residues 1–899 of the encoded protein with S. cerevisiae Rad1, S. pombe rad16, and D. melanogaster MEI-9. The final six residues of the human protein are KGKGKK. The starting positions of two mutations in XP-F patient XP126LO are marked with circles above the human sequence, and the position of a polymorphism is marked with a caret.

consensus translational start site (Kozak, 1987), although an initiation site slightly further upstream is not excluded. The predicted protein has a relative molecular mass of 103 kDa and pI of 6.35.

Homology of the protein to Rad1, rad16, and MEI-9 is most pronounced between residues 699–758 (Figure 1b), a region located in the Rad10 binding domain of Rad1 (Bardwell et al., 1993). In the N-terminal half, several leucine-rich repeats are conserved that may be involved in protein–protein interactions (Schneider and

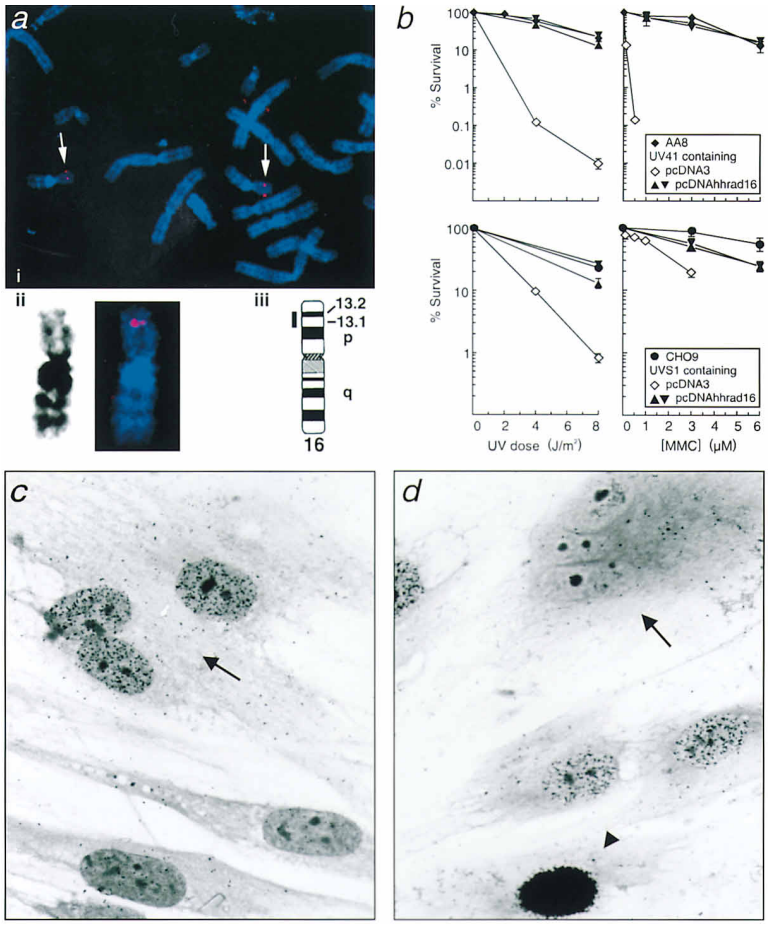

Figure 2. The Cloned cDNA Corrects the Rodent Complementation Group 4 and 11 and XP-F Mutant Phenotypes

(a) (i) Chromosomes (blue) from a single cell showing hybridization to the p arm of each chromosome 16 (red; arrows). (ii) Example of a single chromosome 16 with hybridization signal (left: G-band–like diamidophenylindole pattern shown as an inverse black and white image; right: diamidophenylindole-stained chromosome [blue] with gene signal [red]). (iii) Idiogram of chromosome 16 showing the assigned band position of the *RAD1* homolog.

(b) Survival of UV41 and UVS1 transfectants after treatment with UV and MMC. Bars represent standard errors of mean.

(c) Effect of microinjection of the human Rad1 homolog on UV-induced unscheduled DNA synthesis in XP-F cells; (d), effect of microinjection of anti-ERCC4 antiserum on UV-induced unscheduled DNA synthesis in normal cells. Arrows point to injected polynuclear fibroblasts, obtained by cell fusion of XP126LO (XP-F) or repair-proficient normal fibroblasts, both containing three nuclei. Arrowhead indicates a cell in S phase during incubation with [^{3}H]-thymidine to monitor DNA repair synthesis.

Schweiger, 1991). The relatively poorly conserved central area harbors putative nuclear targeting sequences (Dingwall and Laskey, 1991). Motifs known to be involved in DNA binding or endonuclease function were not found. In a protein sequence property search using the PropSearch algorithm (Hobohm and Sander, 1995), the only high scoring hits found with all four Rad1 family members were eukaryotic homologs of DNA mismatch repair proteins MutS and MutL, human Abr proteins, and mouse Rb.

By means of in situ hybridization, the *RAD1* homolog was localized to human chromosome 16p13.1–13.2 (Figure 2a). This corresponds to the locus of a human repair gene complementing rodent NER mutants of group 4, identified using cell hybrids (Liu et al., 1993) and a genomic clone (Thompson et al., 1994).

Correction of XPF and Rodent Group 4 and 11 Cells by the Human Gene

To determine whether the human homolog could correct one of the rodent ultraviolet (UV)-sensitive mutants, particularly of group 4, the cDNA in a mammalian expression vector (pcDNAhhrad16) was transfected into UV41 (ERCC4[2]), UVS1 (ERCC11[2]), and 43–3B (ERCC1[2]) cells. Stably transfected mass populations of UV41 were obtained that exhibited normal resistance to UV and the cross-linking agent mitomycin C (MMC), to which rodent group 4 (and 1) mutants are extremely sensitive (Figure 2b). This full correction of UV41 was confirmed by the protein expression studies described below and indicates that the cloned cDNA encodes ERCC4. As expected, transfected 43–3B cells did not survive UV selection (data not shown). However, pcDNAhhrad16 also conferred UV- and partial MMC–resistance on UVS1, the only representative of rodent group 11 (Figure 2b), indicating that it is also the group 11 correcting gene. This was surprising, since complementation between UVS1 cells and two different group 4 mutants, UV47 and UV41, has been previously observed by independent laboratories (Busch et al., 1994; Hata et al., 1991). Thus, the two rodent groups represent a unique case of intragenic complementation among mammalian repair genes. The underlying mechanism remains to be elucidated and requires cloning and sequencing of the hamster genes. Interestingly, there is a parallel in S. pombe, in which the *rad16.20* allele, which encodes the N-terminal 45% of the protein, was complemented by a plasmid encoding the C-terminal 60% of the *rad16* gene product (Carr et al., 1994).

To study further the identity of the human gene product, we raised antibodies in rabbits against recombinant C-terminal fragment. The affinity-purified antiserum recognized a protein band migrating on gels at a relative molecular mass of approximately 115 kDa in extracts from Chinese hamster and normal human cells (Figure 3a). Chinese hamster mutant UV41 cells transfected with

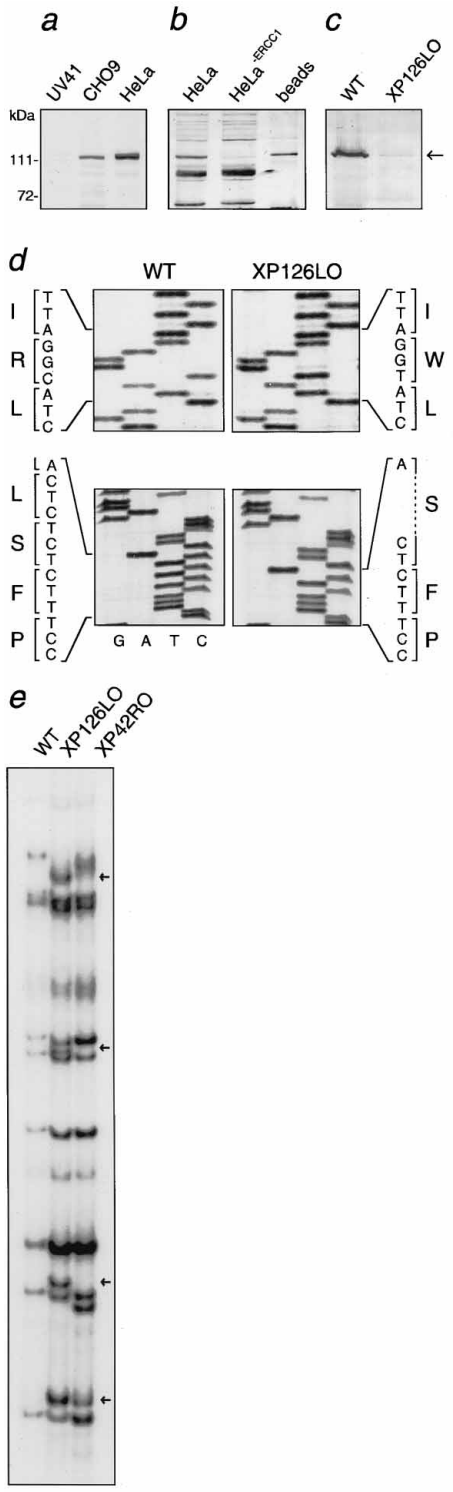

Figure 3. ERCC4 (XPF) Protein

(a) Expression of ERCC4 protein in UV41 compared with normal Chinese hamster ovary CHO9 cells.

(b) Immunoblot showing depletion of ERCC4 from a HeLa total cell extract using anti-ERCC1 antiserum (HeLa^{2ERCC1}) and retention on the antibody beads. The different lanes represent equal amounts of starting material.

(c) Expression of ERCC4 protein in XP126LO (XP-F) cells compared with SV40-transformed normal cells. Arrow indicates ERCC4 (XPF) protein band. A similar relative difference in the amount of XPF protein was found when total cell extracts of primary fibroblasts from normal and several other XP complementation groups were compared with three XP-F fibroblasts. Equal amounts of whole cell extracts were loaded, and blots were incubated with crude (b) or affinity-purified (a), (c), antiserum. Both the hamster and the human XPF protein migrate at 115 kDa.

(d) Sequence showing mutations in the Rad1 homolog.

(e) REF analysis in XP-F patient XP126LO. Shown is the C-terminal part after digestion of DNA from XP-F cells (XP126LO and XP42RO) or normal cells (WT) with EaeI, SacI, and StuI. Aberrant migration is indicated by arrows.

the complementing cDNA regained a band of the same size (data not shown), showing that the cDNA encoded a full-length or near full-length polypeptide. The same protein band was strongly reduced in a HeLa extract depleted for ERCC1 and present in the anti-ERCC1 antiserum-bound fraction (Figure 3b), confirming its presence in the ERCC1 complex.

As outlined in the Introduction, ERCC1 and ERCC4 correcting activities are found in a complex that also harbors correcting activity for XP group F. Although we have previously found reduced levels of ERCC1 protein in cells from XP-F patients (Biggerstaff et al., 1993; van Vuuren et al., 1995), *ERCC1* was explicitly excluded as the gene responsible for XP-F (van Duin et al., 1989). To determine whether the Rad1 homolog is involved in XP group F as well, we microinjected pcDNAhhrad16 into the nucleus of fibroblasts from an XP-F patient. The repair defect was specifically and fully corrected to the level of UV-induced unscheduled DNA synthesis in normal cells (see Figure 2c; Table 1). Moreover, injection of the ERCC4 antiserum into normal human cells caused specific and complete inactivation of NER (Figure 2d) but had no effect on transcription (Table 1) or base excision repair (data not shown), two cellular processes distinct from NER. The inhibitory action of the antibodies was competed by preincubation with the C-terminal ERCC4 fragment but not by bovine serum albumin (data not shown).

Mutations in an XP-F Patient

To obtain direct proof that the Rad1 homolog is responsible for the XP-F repair defect, we searched for mutations in the gene. Restriction endonuclease fingerprinting (REF) indicated sequence alterations in the C-terminal part of both alleles from patient XP126LO (Norris et al., 1988; Figure 3e) and in a second unrelated individual with XP-F. RT–PCR clones (2) of each allele were compared by REF analysis with the original PCR mixture, and both were sequenced to rule out PCR–induced mutations. Sequencing both clones of one allele of XP126LO revealed a 4 nt deletion, TCTC, in a repetitive sequence (TTCTCTCTCA) at position 2281, possibly caused by replication slippage, resulting in a frameshift and a truncated protein of 803 amino acids (Figure 3d). Both clones of the other allele carried a C ! T transition at nucleotide 2377, presumably due to deamination of a methylated cytosine at a CpG site, changing arginine residue 788 (conserved in S. pombe, Drosophila, and human) into a tryptophan (R788W; Figure 3d). In addition

Table 1. Microinjection of cDNA Constructs and Antibodies into Human Cells

Injected substances	Injected cell line	Cellular process assayed	Activity (% of normal)
no injection	XP126LO (XP-F)	NER	15 6 3
pcDNAhhrad16 (*ERCC4* cDNA)	XP126LO (XP-F)	NER	105 6 8
pSVL5E (*ERCC1* cDNA)	XP126LO (XP-F)	NER	15 6 2
no injection	XPCS1BA (XP-B)	NER	7 6 1
pcDNAhhrad16 (*ERCC4* cDNA)	XPCS1BA (XP-B)	NER	8 6 1
preimmune serum	C5RO (normal)	NER	100 6 8
anti-ERCC4 antibodies	C5RO	NER	4 6 1
anti-ERCC4 antibodies	C5RO	transcription	104 6 4

NER activity was determined as UV-induced UDS (see Figure 2), and transcription was measured as [^{3}H]-uridine incorporation. Mean values plus or minus standard errors of the mean are in percent of normal cells.

to these mutational alterations, two sequence polymorphisms were found. One at nucleotide 2090 (A ! G) results in Asp or Gly in the human sequence, at a position coding for Gly in D. melanogaster and S. cerevisiae and Asn in S. pombe. A preliminary analysis to estimate the frequency of this polymorphism showed that the Gly residue was present in more than 10 wild-type alleles examined. The second polymorphism at nucleotide 2487 (C ! T) does not change the amino acid.

We conclude that the Rad1 homolog is indeed responsible for the repair defect in XP group F. In accordance with nomenclature agreements (Lehmann et al., 1994), the name *XPF* is recommended for this gene and XPF for its encoded protein.

Purification of XPF Protein in a Complex with ERCC1

To study the catalytic function of the ERCC1–XPF protein complex, we purified it from cells producing functional His-tagged ERCC1 protein. ERCC1-defective Chinese hamster 43–3B cells were transfected with His-tagged human *ERCC1* cDNA, selected for repair competence, and extensively characterized to ensure stable expression and function of the His-tagged ERCC1. Immunochemical staining confirmed expression of His-ERCC1 protein in the nuclei of transfected 43–3B cells (Figures 4a–4d), and immunoblotting showed that normal amounts of ERCC1 were produced (Figure 4e). The transfected His-ERCC1 fully corrected both the UV and MMC sensitivity of 43–3B cells (Figures 4f and 4g). The use of His-affinity chromatography on chelated nickel columns in combination with five other purification steps resulted in a preparation containing three major polypeptides revealed by silver staining, with relative molecular masses of 42 kDa, 60 kDa, and 115 kDa (Figure 5a). Immunoblotting identified the 42 kDa band as His-tagged ERCC1 and the 115 kDa band as XPF protein, respectively (Figure 5b). The ERCC1 and XPF proteins coeluted at each step and began to separate from the 60 kDa protein and minor contaminants upon gel filtration chromatography (Figure 5a; see different peak fractions for ERCC1–XPF and the 60 kDa band), glycerol gradient sedimentation, or on Reactive Yellow 86 agarose (Figure 5c). These results indicate that the ERCC1 protein complex is a heterodimer of ERCC1 and XPF, consistent with the suggestion of Park et al. (1995). Functional activity was shown by several criteria. The complex could correct the defect in dual incision exhibited by *ERCC1* and *ERCC4* mutant cell extracts, as well as extracts from UVS1 cells (Figure 6a). Human XP-F cell extracts were also corrected by purified complex, as shown in a repair synthesis assay for NER (Figure 6b) and in the dual incision assay. The complex did not contain correcting activity for other mutant cell extracts (Figure 6b). In addition, the complex was active in a fully reconstituted repair system (Aboussekhra et al., 1995; data not shown).

ERCC1–XPF Is a Structure-Specific DNA Endonuclease

To determine whether the purified ERCC1–XPF complex had structure-specific endonuclease activity, we used a partially self-complementary oligonucleotide to form a stem–loop structure consisting of a 22 nt single-stranded loop and a duplex stem of 12 base pairs (Figure 7a). This substrate was end-labeled on either the 39 or 59 terminus, and reaction products were analyzed by comparison to DNA sequencing markers, to map the exact sites of cleavage. The ERCC1–XPF complex specifically cleaved the stem of this substrate 2, 3, and 4 phosphodiester bonds away from the 59 side of the loop (Figure 7a, lanes 2, 3, 6, and 7). These incisions colocalized precisely with those catalyzed by yeast Rad1–Rad10 proteins (Figure 7a, lanes 11, 12, 15, and 16). Conversely, human XPG protein cleaved the substrate on the 39 side of the loop, at the phosphodiester bond on the stem–loop border, and one bond into the stem (Figure 7a, lanes 1 and 8). No cleavage was observed when Mg^{21} was omitted from reaction mixtures.

Several approaches showed that incision activity was intrinsic to the ERCC1–XPF complex. Structure-specific nuclease activity could be directly followed during the last steps (V and VI) of purification and always coeluted with the ERCC1 and XPF polypeptides. Furthermore, agarose beads coupled to anti-ERCC1 antibodies could precipitate the nuclease in an active form on the beads, while beads coupled to preimmune serum could not precipitate active complex (Figure 7b). These findings clearly demonstrate that incision activity is inherent to the ERCC1–XPF complex. When DNA polymerase I (Klenow fragment) and deoxynucleotides were added after cleavage of the stem–loop, the small DNA incision product was quantitatively converted to approximately 36 mer, indicating the presence of an OH group at the 39 terminus of the incision product (Figure 7c).

A "bubble" substrate containing a centrally unpaired region of 30 nt (O'Donovan et al., 1994a) flanked by duplexes of different sequence was also cleaved by

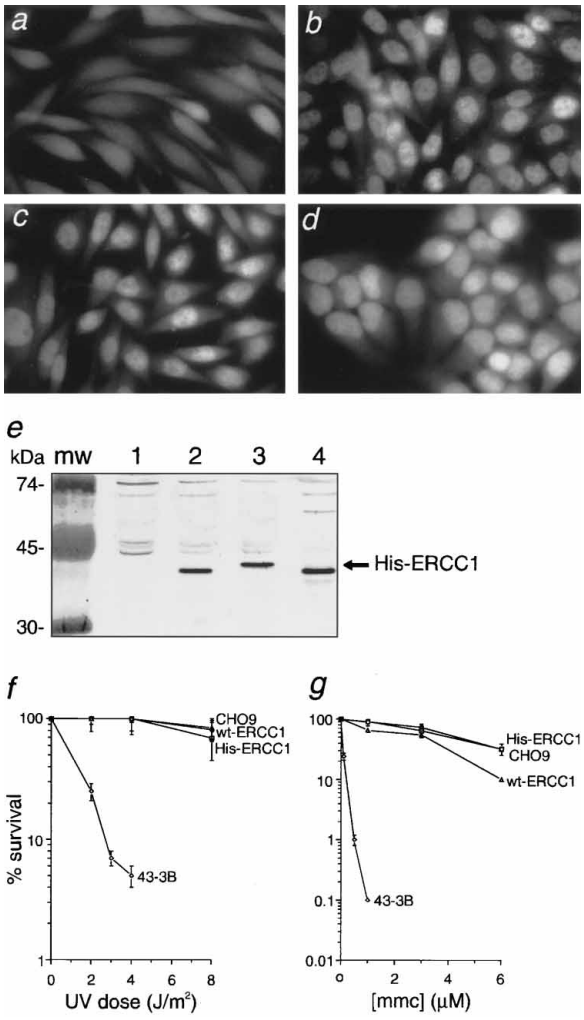

Figure 4. Functional Expression of His-Tagged ERCC1 in Chinese Hamster 43–3B Cells

(a–d) Nuclear localization of His-ERCC1 protein, detected by immunofluorescence microscopy using anti-ERCC1 antibody.
(a) 43–3B cells.
(b) 43–3B plus His-ERCC1.
(c) 43–3B plus wild-type ERCC1.
(d) HeLa.
(e) Immunoblot with anti-ERCC1 antibody, showing ERCC1 expression levels in lane 1, 43–3B; lane 2, 43–3B plus wild-type ERCC1; lane 3, 43–3B plus His-ERCC1; lane 4, HeLa. Similar protein amounts were loaded in the different lanes. Note that the His-tag causes a mobility shift on SDS–polyacrylamide gel electrophoresis and that this anti-ERCC1 antibody does not recognize Chinese hamster ERCC1.
(f, g) Human His-ERCC1 protein fully corrects the UV and MMC sensitivity of 43–3B cells.

ERCC1–XPF, near the 5′ side of the junction between the duplex and unpaired region. However, we did note that ERCC1–XPF cleaved the stem–loop structure more readily than the bubble structure, while XPG preferred the bubble over the stem–loop (data not shown). Additional NER incision step factors such as XPA or RPA were not detectable in the purified preparation and are not required for the structure-specific nuclease activity of ERCC1–XPF with these substrates.

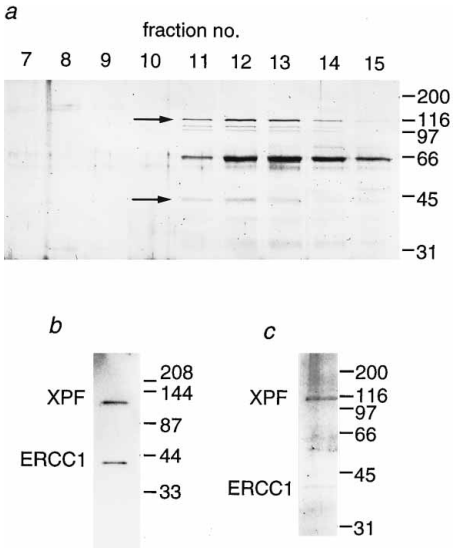

Figure 5. Purified ERCC1–XPF Complex

(a) Fraction V was separated on a Superose 12 gel filtration column. Fractions were analyzed by SDS–polyacrylamide gel electrophoresis and silver-stained. ERCC1 and XPF are indicated by arrows.
(b) Immunoblot of Fraction V, using an antibody raised against full-length ERCC1 and immunopurified antibody (see Figure 3) raised against the C-terminal part of XPF.
(c) Fraction VI after purification on Reactive Yellow 86 agarose.

ERCC1–XPF Makes the 5′ Incision during Repair

These data demonstrate that the ERCC1–XPF complex is a structure-specific endonuclease cleaving one strand of DNA near borders between duplex and single-stranded regions. The polarity of enzymatic cleavage of model substrates strongly suggests that the ERCC1–XPF protein complex makes the 5′ incision during NER. This is indeed the case during repair, as shown in Figure 6a. This assay simultaneously detected excision products resulting from dual incisions as well as uncoupled single incisions in DNA containing a specifically located cisplatin cross-link. Some uncoupled 3′ incisions (without the 5′ incisions) can be observed in normal cell extracts (see Figure 6a, lane 1; see also Matsunaga et al., 1995). In very strong reactions, some uncoupled 5′ incisions also can be detected (Figure 6a, lane 14; see also Moggs et al., 1996). XP-G extracts (defective in 3′ endonuclease activity) or XP-A extracts (missing the damage recognition protein XPA) were defective in incision (Figure 6a, lanes 9, 11, 13). Although ERCC1- or XPF-deficient cell extracts were unable to generate 24–32 nt excision products, fragments corresponding to uncoupled 3′ incisions were still detected (Figure 6a, lanes 2, 4, and 6). The ERCC1 and XP-F cell extracts therefore specifically lack the ability to make the 5′ incision. Addition of purified ERCC1–XPF complex to the extracts restored 5′ incision activity and generated normal excision products (Figure 6a).

Discussion

Identification of the Human *XPF* Gene

In this study, a single human cDNA was isolated that can fully correct the faulty repair in XP-F cells as well

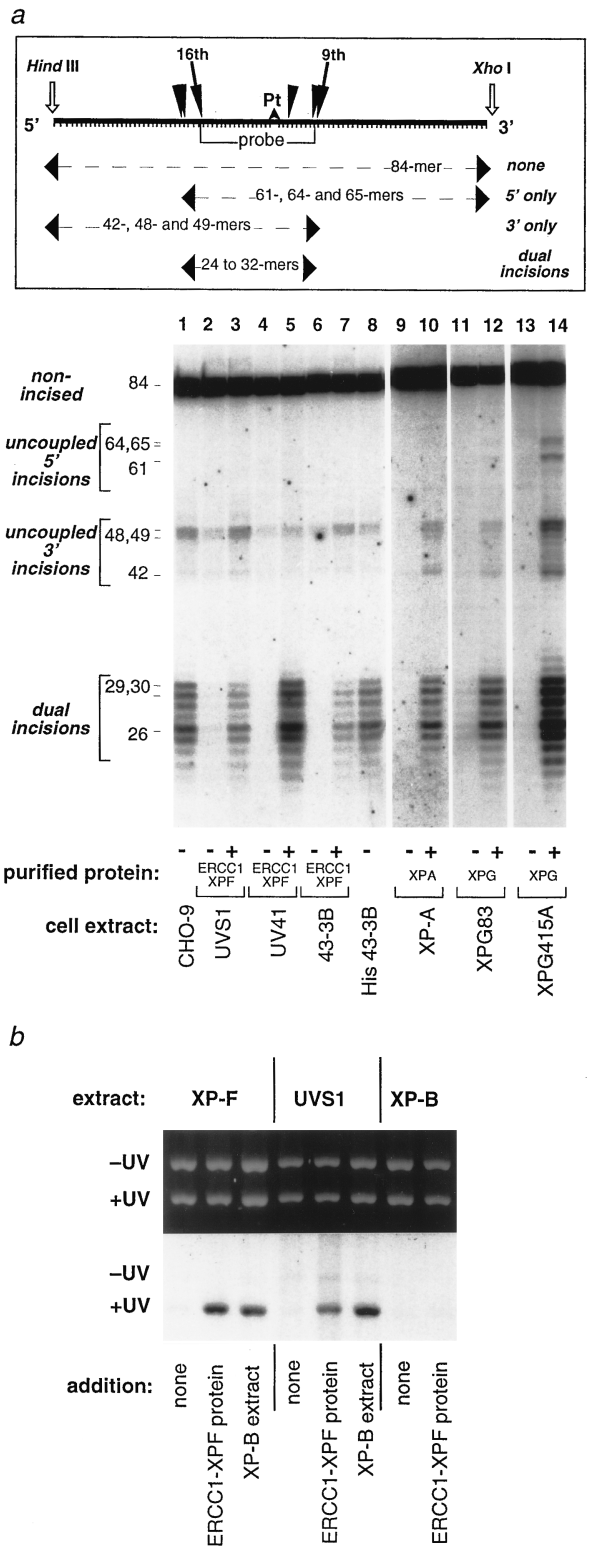

Figure 6. Repair-Correcting Activity of ERCC1–XPF Complex

(a) Autoradiograph of Southern blot. Platinated DNA fragments corresponding to nonincised DNA (84 nt), uncoupled 5′ incisions (61, 64, and 65 nt), uncoupled 3′ incisions (42, 48, and 49 nt), and dual incisions (24–32 nt) were detected after hybridization with a ^{32}P-labeled 27 mer probe complementary to the DNA sequence surrounding the cisplatin cross-link (Moggs et al., 1996), as shown in the schematic diagram. Incision reactions were incubated for 30 min using 200 μg of protein from the cell extracts indicated. The complementing factor added to UVS1 (CHO group 11), UV41 (ERCC4), and 43–3B (ERCC1) cell extracts (lanes 3, 5, and 7, respectively) was ERCC1–XPF (fraction V, 1 μl, approximately 0.1 pmol of complex). Cell extract (200 μg of protein) from 43–3B cells expressing His-tagged ERCC1 was used for lane 8. XPG83 and XPG415A cell extracts were complemented with 50 ng of purified XPG protein (O'Donovan et al., 1994b; lanes 12 and 14, respectively), and XP-A (GM2345) cell extract was complemented with 90 ng of purified XPA protein (Jones and Wood, 1993; lane 10).

(b) Assay for repair synthesis, with human XP-F cell extract, and extracts from Chinese hamster UVS1 cells and 27–1 cells (a hamster XPB/ERCC3 mutant). Repair synthesis is monitored by incubating cell extracts with a mixture of undamaged (2 UV) and UV-damaged (1 UV) circular plasmid DNA in a reaction mixture that includes [α-^{32}P]dATP (Wood et al., 1995). Lanes 1, 2, 4, 5, 7, and 8 had 100 μg of the indicated extract (CFII fraction); lanes 3 and 6 had 50 μg of each CFII fraction. Purified ERCC1–XPF protein (fraction V, 1 μl) was added in lanes 2, 5, and 8.

as in rodent group 4 and 11 cells. Although this has been suggested previously, based on indirect indications (Biggerstaff et al., 1993; van Vuuren et al., 1993; Reardon et al., 1993; Park et al., 1995), this study provides a unique demonstration that *XPF*, *ERCC4*, and the group 11 defects are allelic. Intriguingly, the correspondence between rodent groups 4 and 11 is the only known case of intragenic complementation between mammalian NER mutants. The cloning of *XPF* completes the isolation of the set of XP genes that are required for the core process of NER in mammalian cells. The gene is also the final one correcting the six original complementation groups of rodent repair mutants that have been classified by Busch, Thompson, and coworkers (Busch et al., 1989).

We find that the encoded XPF (ERCC4) protein is intrinsic to an active ERCC1-containing protein complex. The mutations located in the examined XP-F cells occur in the region expected to be involved in ERCC1 binding, based on studies of the homologous yeast complex (Bardwell et al., 1993). We have noted that ERCC1 mutations interfering with complex formation result in rapid degradation of ERCC1 and that the degree of sensitivity to UV light and MMC depends on the amount of ERCC1 complex expressed (our unpublished data). The reduced amount of XPF protein detected in extracts of XP-F cells (Figure 3a), 43–3B, and UVS1 rodent cells (data not shown) closely resembles the strongly reduced levels of ERCC1 protein in these cells that we reported earlier (Biggerstaff et al., 1993; van Vuuren et al., 1995) and suggests that complex formation is required for the stability of the XPF component as well. In rodent mutants, hypersensitivity to MMC occurs only at very low levels of ERCC1 (our unpublished data). The residual amount of ERCC1–XPF complex present in XP-F cells may account for their moderate sensitivity to MMC and the slow extended repair characteristic of XP-F (Zelle et al., 1980).

XPF Protein Is a Subunit of the Nuclease That Makes the 5′ Incision

These studies with purified ERCC1–XPF show that the complex has an intrinsic structure-specific endonucle-

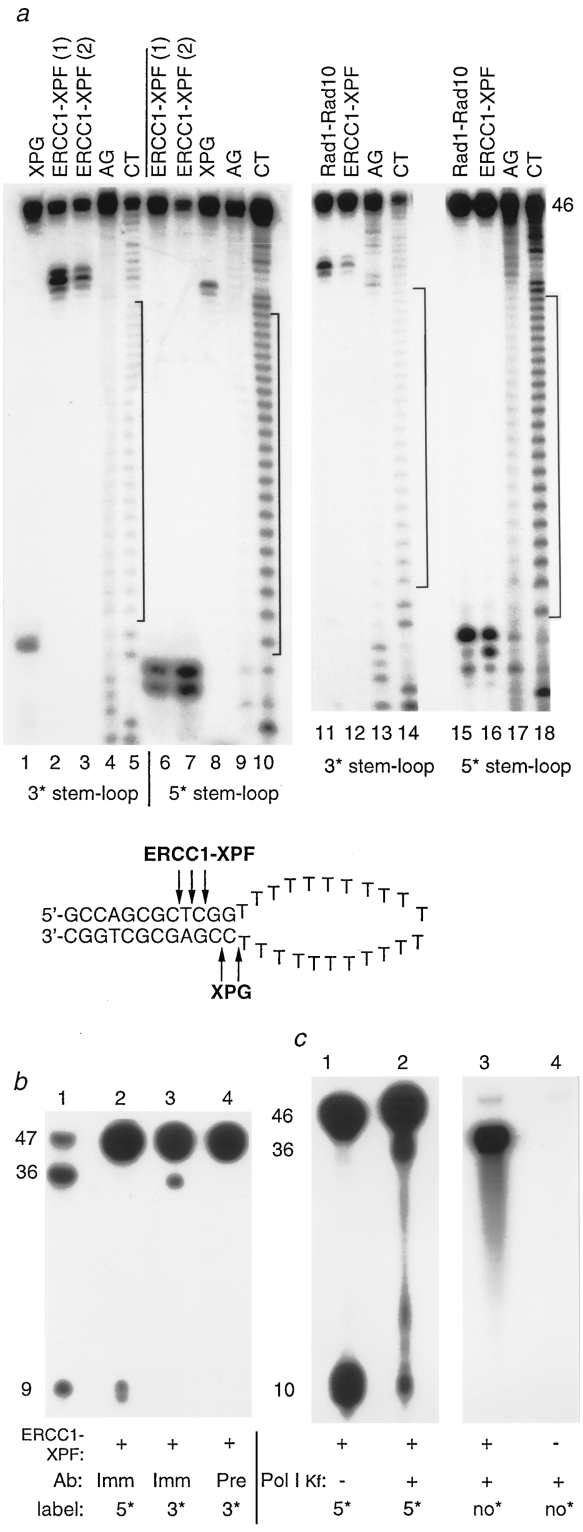

Figure 7. The ERCC1–XPF Complex Is a Structure-Specific Endonuclease

(a) The structure of the stem–loop substrate is shown below the gel. Arrows indicate the sites of cleavage for the indicated enzymes, as determined from Maxam-Gilbert sequencing ladders. For 59 labeling, Maxam-Gilbert products migrate approximately 1.5 nt faster than the corresponding nuclease products. The 22 T residues are indicated by brackets. Lanes 1–5, 39-labeled stem–loop with lane 1, XPG (50 ng); lanes 2 and 3, ERCC1–XPF (purified fraction V, 1 and 2 ml, respectively); lanes 4 and 5, Maxam-Gilbert G 1 A and C 1 T sequencing ladders. Lanes 6–10, 59-labeled stem–loop with lanes 6 and 7, ERCC1–XPF (purified fraction V, 1 and 2 ml, respectively); lane 8, XPG (50 ng); lanes 9 and 10, G 1 A and C 1 T sequencing ladders. Lanes 11–14, 39-labeled stem–loop with: lane 11, Rad1 (100 ng) and Rad10 (25 ng); lane 12, ERCC1–XPF (1 ml, fraction V); lanes 13 and 14, Maxam Gilbert G 1 A and C 1 T sequencing ladders. Lanes 15–18, same as 11–14 with 59-labeled stem-loop.

(b) Nuclease activity isolated on antibody-affinity beads. Lane 1, 59-[^{32}P]-labeled marker oligonucleotides; lane 2, 59-labeled stem–loop plus affinity-purified anti-ERCC1 antibody-beads (Imm) preincubated with purified ERCC1–XPF; lane 3, as lane 2 but with 39-labeled stem–loop; lane 4, as lane 3 but with preimmune antibody-beads (Pre) preincubated with purified ERCC1–XPF.

(c) Analysis of the 39 end of the cleavage product. Lane 1, 59-[^{32}P]-labeled stem–loop plus purified ERCC1–XPF complex; lane 2, 59-labeled stem–loop cleaved with ERCC1–XPF, followed by incubation with the Klenow fragment of E. coli DNA polymerase I (Pol I Kf) and unlabeled dNTPs. Lane 3, unlabeled stem–loop cleaved with ERCC1–XPF and then extended with Pol I (Kf) and [^{32}P]-labeled dNTPs; lane 4, control reaction in which unlabeled stem–loop was incubated with Pol I (Kf) and [^{32}P]-labeled dNTPs.

ase activity. There are significant parallels with the homologous nuclease complex formed by the Rad1–Rad10 proteins in S. cerevisiae. The yeast complex consists of two subunits that are sufficient to perform incision (Tomkinson et al., 1993, 1994; Sung et al., 1993; Bardwell et al., 1994). Our data, including the findings that the 115 kDa component of the human is XPF and is equivalent to ERCC4 and ERCC11, are completely consistent with an heterodimeric composition in mammalian cells as well. Moreover, the cleavage specificities of ERCC1–XPF and Rad1–Rad10 are identical, both on the stem–loop structure (Figure 7a) and on other substrates. The polarity of cleavage for these enzymes is the opposite of that mediated by XPG nuclease, and the incision sites of ERCC1–XPF are slightly further from the stem–loop junction than those mediated by XPG. Although it was known that XPG and Rad1–Rad10 cleaved near the border of single-stranded and duplex DNA, these data represent the only example in which cleavage sites have been definitively mapped at nucleotide resolution.

In addition, experiments with a specifically placed cisplatin-DNA adduct showed directly that the structure-specific endonuclease activity of ERCC1–XPF is responsible for the 59 incision during the nucleotide excision repair reaction. Finally, it was determined that the product resulting from cleavage by the human enzyme has a 39 OH group, so that gap-filling DNA synthesis can start at the 59 incision site without additional DNA modifications. The fragments produced by dual incision still retain a 59 phosphate (Moggs et al., 1996), indicating that ERCC1–XPF makes the 59 nick without further processing. Since only the damaged DNA strand is cleaved during nucleotide excision repair, it is likely that lesion-dependent positioning of other incision components such as XPA, RPA, TFIIH, and XPC restricts the action of the two structure-specific repair endonucleases (XPG and ERCC1–XPF) to the damaged strand.

In contrast to the above findings and to those in yeast, a purified preparation containing ERCC1 and a 115 kDa

polypeptide from HeLa cells was reported to lack any structure-specific DNA endonuclease activity on a bubble substrate, acting instead as a weak single-stranded endonuclease (Park et al., 1995). However, the absence of cleavage in the single-stranded regions of the stem–loop or bubble structures in our assays shows that the ERCC1–XPF complex does not cut single-stranded DNA indiscriminately.

Consequences of XPF–ERCC1 Complex Inactivation

In the mouse, full inactivation of the *ERCC1* gene results in a severe phenotype causing early death (McWhir et al., 1993; G. Weeda and J. H. J. H., unpublished data). This extreme phenotype suggests that the mammalian ERCC1–XPF complex has a function in addition to NER. In yeast, the homologous Rad1–Rad10 proteins are known to engage in a pathway of mitotic recombination by single-stranded DNA annealing (Ivanov and Haber, 1995; Davies et al., 1995). The enzymatic activity demonstrated here for ERCC1–XPF suggests that this complex would also be suitable for such a recombination process in mammalian cells. Impairment of the recombination function of the ERCC1–XPF complex (which is presumably required for repair of MMC–induced DNA cross-links) may underlie the severe phenotype of ERCC1 null mice.

In contrast, the known XP-F patients have relatively mild clinical symptoms, and some are reported to survive into their sixties (Yamamura and Ichihashi, 1989). It remains to be seen whether all group F individuals with the sun-sensitive disorder xeroderma pigmentosum express a low level of ERCC1–XPF complex and whether a complete absence of ERCC1–XPF is compatible with human viability.

Experimental Procedures

Isolation of the Human *XPF* cDNA

The 59 part of the gene was isolated by using the S. pombe rad16 and S. cerevisiae Rad1 sequences to search a database of human expressed sequence tag sequences (Adams et al., 1991, 1995). Of two expressed sequence tag clones detected, the longer (HGS238927) was from a human testis cDNA library. The insert of approximately 2.1 kb encoded a polypeptide with homology to the N-terminal part of rad16, Rad1, and MEI-9. The HGS238927 insert was used to screen a human testis cDNA library by hybridization, which identified a clone (rad16o26) with additional 59 terminal sequence. RACE on multiple cDNA libraries confirmed the sequence of rad16o26 and the presumed AUG initiation codon.

To isolate the 39 part of the gene, numerous degenerate primers were designed for regions in which the *RAD1*, *rad16*, and D. melanogaster *mei-9* gene products show sequence conservation. In positions where one species differed from two others, the majority rule was followed. At positions where all three differed, the residue in the species most closely related to mammals was utilized. Conditions for PCR amplification were optimized using S. pombe cDNA as starting material. Products were evaluated further only if they corresponded to the predicted size. One appropriate primer pair was 59-TIGTIGAT/CATGA/CGIGAA/GTT-39 and 59-CIGGIGTIAA/GIATA/GTAA/CTCICCIAC-39. The protocol for this PCR amplification was 4 min at 948C (hot start), followed by 35 cycles of 1.5 min at 948C, 1.5 min at 418C, and 1.5 min at 728C. The final cycle was concluded with 10 min at 728C. Reaction mixtures in 60 mM Tris–HCl buffer (pH 8.5) contained 15 mM $(NH_4)_2SO_4$, 2.5 mM $MgCl_2$, 0.2 mM dNTPs, 100 pmol primers, and SuperTaq (HT Biotechnology, Ltd.) in a Perkin Elmer Cetus DNA thermocycler. RNA from a non–XP-F primary fibroblast cell line or HeLa cells was used for random hexamer-primed RT–cDNA synthesis using standard conditions. After verification that the amplified product was derived from a human gene with clear homology to *RAD1*, the PCR product was used as a probe to identify a clone from a human testis cDNA library that encoded a polypeptide with homology to the C-terminal part of the yeast and fly proteins. The insert was cloned into pBluescript, yielding pBSChhrad16. The 59 end of the pBSChhrad16 clone overlapped by 338 bp with the 39 end of the HGS238927 sequence.

To construct a complete cDNA, we first subcloned a 1636 bp BsaAI fragment from pBSChhrad16 into the pBluescript vector carrying HGS238927, to obtain pBSHGSChhrad16. A human fibroblast cDNA library (Keyse and Emslie, 1992) was used in a PCR to obtain a fragment containing the most N-terminal sequence flanked by SacI and EagI sites. This PCR fragment was SacI–EagI–digested and separately subcloned into the pBluescript vector carrying HGS238927. An 801 bp BamHI–XbaI fragment from the latter construct was inserted into pBSHGSChhrad16 to create a plasmid containing the complete coding sequence, pBShhrad16. The sequence of the assembled cDNA was determined on both strands and matched all partial cDNA clones and RACE sequences. For expression in mammalian cells, a 2940 bp NotI–ApaI fragment from pBShhrad16 was cloned into pcDNA3 (InVitrogen), yielding pcDNAhhrad16.

Mutation Analysis

The gene was amplified in two overlapping segments in an RT–PCR using total RNA isolated from XP-F and normal cells. For REF analysis, the products were digested with different sets of restriction enzymes in the presence of shrimp alkaline phosphatase. Pooled digestions were 59-end-labeled with [^{32}P] by T4 polynucleotide kinase, denatured, and single strands separated based on their conformation, on a nondenaturing polyacrylamide gel containing 5% glycerol and run at 48C (Liu and Sommer, 1995). Fragments of the two alleles were subcloned and sequenced from XP126LO, XP42RO (both XP-F cell lines), and normal primary fibroblasts (WT).

Fluorescence In Situ Hybridization

The *RAD1* homolog cDNA was nick-translated using Digoxigenin-dUTP (Boehringer Mannheim), and fluorescence in situ hybridization was done as detailed (Johnson et al., 1991). Individual chromosomes were counterstained with diamidophenylindole, and images were recorded using a charged coupled-device camera and analyzed using ISEE software (Inovision Corp.). Spreads (approximately 20) were analyzed by eye, and most had a doublet signal characteristic of genuine hybridization on at least one chromosome 16. Doublet signal was not detected on any other chromosomes. Individual chromosomes (10) were analyzed in detail using a combination of fractional length measurements and fluorescence banding combined with high resolution image analysis.

Selection and Characterization of 43–3B His-ERCC1 Cells

A tag sequence was introduced at the 39 end of *ERCC1* by PCR methods, to encode a fusion protein consisting of normal full-length human *ERCC1* cDNA followed by Gly–Gly–Ser, a thrombin cleavage site, and six His residues. This construct (pSVL–ERCC1-His) was transfected into 43–3B cells (Wood and Burki, 1982), and repair-competent transformants were selected after repeated UV irradiation (4.6 J/m^2). The number of cells surviving treatment with UV or MMC (1 hr) was measured as [^{3}H]-thymidine incorporation 6 days after exposure. Proliferating cells were pulse-labeled with tritiated thymidine (1 hr), followed by a chase (1 hr) to deplete radioactive precursor pools. Cells were lysed in 0.05 M NaOH and transferred to scintillation-counting vials. Survival was calculated as the average ratio of incorporated radiolabel in treated duplicates to that in four untreated control dishes.

Correction of Rodent Mutants by Transfection

pcDNA3 (neo) and pcDNAhhrad16 were transfected into UV41, UVS1, and 43–3B cells using lipofectin, as described previously (Troelstra et al., 1992). Stable transfected mass populations were selected on G418 (800 mg/ml) and UV (UV41 3 3 8 J/m^2 and UVS1 3 3 18 J/m^2). Subsequently, 500–5000 cells were seeded in 30 mm

wells and either UV-irradiated or incubated with the cross-linking agent MMC for 1 hr. Survival was measured as [^{3}H]-thymidine incorporation 7 days after exposure.

Microinjection

pcDNAhhrad16 or anti-ERCC4 antiserum was injected into one of the nuclei of XP126LO (XP-F) homopolykaryons or into the cytoplasm of C5RO (normal human primary fibroblasts) homopolykaryons. Repair activity was determined after 24 hr by UV-induced (15 J/m^2) incorporation of [^{3}H]-thymidine and autoradiography as described (Vermeulen et al., 1994). The number of silver grains above the nuclei is a measure of the level of unscheduled DNA synthesis and reflects the cellular repair capacity.

Immunological Methods

An Escherichia coli expression construct was made coding for a GST–ERCC4 fusion protein containing the 391 C-terminal residues present in pBSChhrad16. Antibodies raised against fusion protein were isolated on a glutathione column and affinity-purified. Immunofluorescence, SDS–polyacrylamide gel electrophoresis, and immunoblotting were performed according to standard procedures (Sambrook et al., 1989), using polyclonal antibodies against human ERCC1 and ERCC4. A HeLa whole-cell extract was depleted for ERCC1 using anti-ERCC1 antiserum coupled to protein A beads.

Isolation of ERCC1–XPF Protein Complex

ERCC1–XPF complex was isolated from 43–3B His-ERCC1 cells, monitoring purification by immunoblotting using an antibody against ERCC1 and by repair-correcting activity. A nuclear extract (Masutani et al., 1994) was prepared from 1.4 3 10^{11} frozen cells and dialyzed against buffer A (20 mM HEPES–KOH [pH 7.5], 0.2 mM EDTA, 2 mM $MgCl_2$, 10% glycerol, 0.2 mM 4-(2-aminoethyl)benzenesulfonyl fluoride, 5 mM b-mercaptoethanol) containing 0.15 M KCl and 10 mg/ml of aprotinin. The extract (1.5 g) was loaded onto a phosphocellulose column (Whatman P11; 300 ml) equilibrated in the same buffer. The flow-through fraction contained the incision protein RPA and proteins not needed for NER (Shivji et al., 1992; Biggerstaff et al., 1993).

Bound proteins (Fraction I, 600 mg protein) were eluted with buffer A containing 1.0 M KCl, supplemented with 1 mM imidazole (Fluka), and applied directly onto a Ni^{21}–NTA agarose column (Qiagen; 25 ml). The column was washed at 25 ml/hr and eluted sequentially with buffer B (20 mM HEPES–KOH [pH 7.5], 2 mM $MgCl_2$, 10% glycerol, 0.2 mM 4-(2-aminoethyl)benzenesulfonyl fluoride, 5 mM b-mercaptoethanol, 0.5 M KCl) containing 1 mM, 5 mM (pH 6.6), 20 mM (pH 7.5), and 100 mM imidazole (pH 7.5). ERCC1 was eluted in the last fraction (Fraction II, 35 mg protein), supplemented with 0.02% NP-40 and 1 mM potassium phosphate, and loaded onto a hydroxyapatite column (Bio-Rad; 3 ml). The column was washed with buffer C (25 mM HEPES–KOH [pH 7.8], 10% glycerol, 0.2 mM 4-(2-aminoethyl)benzenesulfonyl fluoride, 2 mM dithiothreitol, 0.02% NP-40) containing 5 mM potassium phosphate and 0.5 M KCl. ERCC1 was eluted in buffer C containing 30 mM potassium phosphate and 0.5 M KCl (Fraction III, 10 mg). The fraction was dialyzed against buffer C plus 1 mM EDTA and 50 mM KCl, filtered through a 0.45 mm filter (Millipore), and applied onto an FPLC Mono Q HR 5/5 column (Pharmacia). A gradient of 50–300 mM KCl in buffer C was applied, and 0.5 ml fractions were collected; ERCC1 eluted at about 0.2 M KCl. ERCC1-containing peak fractions (Fraction IV, 4 ml) were pooled, diluted to 50 mM KCl with buffer C, loaded onto an FPLC Mono S column, and eluted with a gradient of 50–300 mM KCl. Peak fractions (Fraction V, 1.5 ml; approximately 0.1 pmol ERCC1 complex/ml) eluted at approximately 0.22 M KCl. A SMART system (Pharmacia) was used for the Superose 12 gel filtration in Figure 5a. For Figure 5c, 20 ml of fraction V was diluted 1:2 in buffer C and added to 10 ml of swollen Reactive Yellow 86 agarose (Sigma) to give 50 ml in 25 mM HEPES–KOH (pH 7.8), 10% glycerol, 2 mM dithiothreitol, and 100 mM KCl. After 1 hr at 48C, the suspension was centrifuged and 30 ml of supernatant loaded onto the gel.

In Vitro DNA Repair and Nuclease Assays

The assay for dual incision was as described (Moggs et al., 1996), except that the plasmid was cleaved with HindIII and XhoI before detection by Southern hybridization. Repair synthesis assays used CFII protein fraction from the indicated cells, purified RPA, and purified proliferating cell nuclear antigen, as previously described (Biggerstaff et al., 1993).

Nuclease reaction mixtures (15 ml) contained 0.2–0.5 ng of stem–loop DNA and the indicated proteins in buffer as described (O'Donovan et al., 1994a) for Figure 7a, lanes 1–10, or in buffer D (50 mM Tris–HCl [pH 8.0], 10 mM $MgCl_2$, 100 mg/ml of bovine serum albumin, and 0.5 mM b-mercaptoethanol) for lanes 11–18. After incubation at 258C for 2 hr, 15 ml of 90% formaldehyde was added, and samples were heated at 958C and loaded onto denaturing 12% polyacrylamide gels. Products were visualized by autoradiography or a phosphorimager. Maxam-Gilbert A 1 G and C 1 T reactions were carried out on the 39- and 59-labeled stem–loop substrates in order to locate the sites of enzymatic cleavage. For immunoprecipitation, affinity-purified anti-ERCC1 antiserum (30 ml) was coupled to 10 ml of protein G beads, and beads were extensively washed and incubated with the indicated amount of ERCC1–XPF complex in 20 ml of buffer D at 48C. After 2 hr, beads were washed twice with 100 ml of buffer D and added to the nuclease reaction mixture. Samples were then loaded on a denaturing 20% polyacrylamide gel. For the end-labeling analysis in Figure 7c, reaction mixtures containing 59-labeled (lanes 1 and 2) or unlabeled (lanes 3 and 4) stem–loop substrate were incubated for 16 hr at 168C, with or without ERCC1–XPF complex (1 ml of fraction V) as indicated. In lane 2, 1 ml of 5 mM dNTPs plus 1 U E. coli DNA pol I (Klenow fragment) was added for a further 30 min. For lanes 3 and 4, 5 nmol of dGTP, dCTP, and dTTP and 2 nmol of [a-^{32}P]dATP were added for 30 min, followed by a 90 min chase with 10 nmol of unlabeled dATP.

Acknowledgments

Correspondence should be addressed to R. D. W. We thank the members of our laboratories for advice and reagents; A. A. Davies, R. Sowdhamini, W. Vermeulen, and T. Yagi for discussions; and E. C. Friedberg for the Rad1–Rad10 proteins. We thank A. J. van Vuuren, A. de Klein, R. van Os, H. Odijk, and J. de Wit for help with the experiments. This work was supported by the Imperial Cancer Research Fund, the Human Frontiers of Science Programme, the Dutch Scientific Organisation (NWO, Foundation for Chemical Research), and the European Community Human Capital and Mobility Programme.

References

Aboussekhra, A., Biggerstaff, M., Shivji, M.K.K., Vilpo, J.A., Moncollin, V., Podust, V.N., Protić, M., Hübscher, U., Egly, J.-M., and Wood, R.D. (1995). Mammalian DNA nucleotide excision repair reconstituted with purified protein components. Cell *80*, 859–868.

Adams, M.D., Kelley, J.M., Gocayne, J.D., Dubnick, M., Polymeropoulos, M.H., Xiao, H., Merril, C.R., Wu, A., Olde, B., Moreno, R.F., Kerlavage, A.R., McCombie, W.R., and Venter, J.C. (1991). Complementary DNA sequencing: expressed sequence tags and human genome project. Science *252*, 1651–1656.

Adams, M.D., Kerlavage, A.R., Fleischmann, R.D., Fuldner, R.A., Buit, C.J., Lee, N.H., Kirkness, E.F., Weinstock, K.G., and others (1995). Initial assessment of human gene diversity and expression patterns based upon 83 million nucleotides of cDNA sequence. Nature *377S*, 3–174.

Bardwell, A.J., Bardwell, L., Johnson, D.K., and Friedberg, E.C. (1993). Yeast DNA recombination and repair proteins Rad1 and Rad10 constitute a complex in vivo mediated by localized hydrophobic domains. Mol. Microbiol. *8*, 1177–1188.

Bardwell, A.J., Bardwell, L., Tomkinson, A.E., and Friedberg, E.C. (1994). Specific cleavage of model recombination and repair intermediates by the yeast Rad1–Rad10 DNA endonuclease. Science *265*, 2082–2085.

Biggerstaff, M., Szymkowski, D.E., and Wood, R.D. (1993). Cocorrection of the ERCC1, ERCC4, and xeroderma pigmentosum group F DNA repair defects *in vitro*. EMBO J. *12*, 3685–3692.

Busch, D., Greiner, C., Lewis, K., Ford, R., Adair, G., and Thompson, L. (1989). Summary of complementation groups of UV-sensitive CHO

cell mutants isolated by large-scale screening. Mutagenesis *4*, 349–354.

Busch, D., Greiner, C., Rosenfeld, K.L., Ford, R., Dewit, J., Hoeijmakers, J.H.J., and Thompson, L.H. (1994). Complementation group assignments of moderately UV-sensitive CHO mutants isolated by large-scale screening (FAECB). Mutagenesis *9*, 301–306.

Carr, A., Schmidt, H., Kirchhoff, S., Muriel, W., Sheldrick, K., Griffiths, D., Basmacioglu, C., Subramani, S., Clegg, M., and Nasim, A. (1994). The *rad16* gene of *Schizosaccharomyces pombe*—a homolog of the *Rad1* gene of *Saccharomyces cerevisiae*. Mol. Cell Biol. *14*, 2029–2040.

Davies, A.A., Friedberg, E.C., Tomkinson, A.E., Wood, R.D., and West, S.C. (1995). Role of the RAD1 and RAD10 proteins in nucleotide excision repair and recombination. J. Biol. Chem. *270*, 24638–24641.

Dingwall, C., and Laskey, R.A. (1991). Nuclear targeting sequences—a consensus? Trends Biochem. Sci. *16*, 478–481.

Friedberg, E.C., Walker, G.C., and Siede, W. (1995). DNA Repair and Mutagenesis. (Washington, D.C.: ASM Press).

Habraken, Y., Sung, P., Prakash, L., and Prakash, S. (1995). Structure-specific nuclease activity in yeast nucleotide excision-repair protein Rad2. J. Biol. Chem. *270*, 30194–30198.

Harrington, J.J., and Lieber, M.R. (1994). Functional domains within FEN-1 and Rad2 define a family of structure-specific endonucleases—implications for nucleotide excision repair. Genes Dev. *8*, 1344–1355.

Hata, H., Numata, M., Tohda, H., Yasui, A., and Oikawa, A. (1991). Isolation of two chloroethylnitrosourea-sensitive Chinese hamster cell lines. Cancer Res. *51*, 195–198.

Hobohm, U., and Sander, C. (1995). A sequence property approach to searching protein databases. J. Mol. Biol. *251*, 390–399.

Hoeijmakers, J.H.J. (1994). Human nucleotide excision repair syndromes: molecular clues to unexpected intricacies. Eur. J. Cancer *30A*, 1912–1924.

Huang, J.C., Svoboda, D.L., Reardon, J.T., and Sancar, A. (1992). Human nucleotide excision nuclease removes thymine dimers from DNA by incising the 22nd phosphodiester bond 59 and the 6th phosphodiester bond 39 to the photodimer. Proc. Natl. Acad. Sci. USA *89*, 3664–3668.

Ivanov, E.L., and Haber, J.E. (1995). Rad1 and rad10, but not other excision-repair genes, are required for double-strand break-induced recombination in *Saccharomyces cerevisiae*. Mol Cell Biol *15*, 2245–2251.

Johnson, C.V., Singer, R.H., and Lawrence, J.B. (1991). Fluorescent detection of nuclear RNA and DNA: implications for genome organization. Meth. Cell Biol. *35*, 73–99.

Jones, C.J., and Wood, R.D. (1993). Preferential binding of the xeroderma pigmentosum group A complementing protein to damaged DNA. Biochemistry *32*, 12096–12104.

Keyse, S.M., and Emslie, E.A. (1992). Oxidative stress and heat shock induce a human gene encoding a protein-tyrosine phosphatase. Nature *359*, 644–646.

Kozak, M. (1987). An analysis of 59-noncoding sequences from 699 vertebrate messenger RNAs. Nucl. Acids Res. *15*, 8125–8148.

Lehmann, A.R., Bootsma, D., Clarkson, S.G., Cleaver, J.E., McAlpine, P.J., Tanaka, K., Thompson, L.H., and Wood, R.D. (1994). Nomenclature of human DNA repair genes. Mutat. Res. *315*, 41–42.

Liu, P., Siciliano, J., White, B., Legerski, R., Callen, D., Reeders, S., Siciliano, M.J., and Thompson, L.H. (1993). Regional mapping of human DNA excision-repair gene *ERCC4* to chromosome 16p13.13–p13.2. Mutagenesis *8*, 199–205.

Liu, Q.Q., and Sommer, S.S. (1995). Restriction endonuclease fingerprinting (REF): a sensitive method for screening mutations in long, contiguous segments of DNA. Biotechniques *18*, 470–477.

Masutani, C., Sugasawa, K., Yanagisawa, J., Sonoyama, T., Ui, M., Enomoto, T., Takio, K., Tanaka, K., van der Spek, P.J., Bootsma, D., Hoeijmakers, J.H.J., and Hanaoka, F. (1994). Purification and cloning of a nucleotide excision repair complex involving the xeroderma pigmentosum group C protein and a human homolog of yeast RAD23. EMBO J. *13*, 1831–1843.

Matsunaga, T., Mu, D., Park, C.H., Reardon, J.T., and Sancar, A. (1995). Human DNA–repair excision nuclease: analysis of the roles of the subunits involved in dual incisions by using anti-XPG and anti-ERCC1 antibodies. J. Biol. Chem. *270*, 20862–20869.

McWhir, J., Selfridge, J., Harrison, D.J., Squires, S., and Melton, D.W. (1993). Mice with DNA repair gene (ERCC-1) deficiency have elevated levels of p53, liver nuclear abnormalities, and die before weaning. Nature Genet. *5*, 217–224.

Moggs, J.G., Yarema, K.J., Essigmann, J.M., and Wood, R.D. (1996). Analysis of incision sites produced by human cell extracts and purified proteins during nucleotide excision repair of a 1,3-intrastrand d(GpTpG)-cisplatin adduct. J. Biol. Chem. *271*, 7177–7186.

Norris, P.G., Hawk, J.L.M., and Giannelli, F. (1988). Xeroderma pigmentosum complementation group F in a non-Japanese patient. J. Am. Acad. Dermatol. *18*, 1185–1188.

O'Donovan, A., Davies, A.A., Moggs, J.G., West, S.C., and Wood, R.D. (1994a). XPG endonuclease makes the 39 incision in human DNA nucleotide excision repair. Nature *371*, 432–435.

O'Donovan, A., Scherly, D., Clarkson, S.G., and Wood, R.D. (1994b). Isolation of active recombinant XPG protein, a human DNA repair endonuclease. J. Biol. Chem. *269*, 15965–15968.

Park, C.H., Bessho, T., Matsunaga, T., and Sancar, A. (1995). Purification and characterization of the XPF–ERCC1 complex of human DNA–repair excision nuclease. J. Biol. Chem. *270*, 22657–22660.

Reardon, J.T., Thompson, L.H., and Sancar, A. (1993). Excision repair in man and the molecular basis of xeroderma pigmentosum syndrome. In Cold Spring Harbor Symposia on Quantitative Biology, B. Stillman and B. Alberts, eds. (Cold Spring Harbor, New York: Cold Spring Harbor Laboratory Press), pp. 605–617.

Reynolds, P., Prakash, L., and Prakash, S. (1987). Nucleotide sequence and functional analysis of the RAD1 gene of *S. cerevisiae*. Mol. Cell. Biol. *7*, 1012–1120.

Sambrook, J., Fritsch, E., and Maniatis, T. (1989). Molecular Cloning: A Laboratory Manual. (Cold Spring Harbor, New York: Cold Spring Harbor Laboratory Press.)

Schneider, R., and Schweiger, M. (1991). The yeast DNA–repair proteins RAD1 and RAD7 share similar putative functional domains. FEBS Lett. *283*, 203–206.

Sekelsky, J.J., McKim, K.S., Chin, G.M., and Hawley, R.S. (1995). The *Drosophila* meiotic recombination gene mei-9 encodes a homolog of the yeast excision-repair protein RAD1. Genetics *141*, 619–627.

Shivji, M.K.K., Kenny, M.K., and Wood, R.D. (1992). Proliferating cell nuclear antigen is required for DNA excision repair. Cell *69*, 367–374.

Sung, P., Reynolds, P., Prakash, L., and Prakash, S. (1993). Purification and characterization of the *Saccharomyces cerevisiae RAD1–RAD10* endonuclease. J. Biol. Chem. *268*, 26391–26399.

Thompson, L.H., Brookman, K.W., Weber, C.A., Salazar, E.P., Reardon, J.T., Sancar, A., Deng, Z.M., and Siciliano, M.J. (1994). Molecular cloning of the human nucleotide excision-repair gene *ERCC4*. Proc. Natl. Acad. Sci. USA *91*, 6855–6859.

Tomkinson, A.E., Bardwell, A.J., Bardwell, L., Tappe, N.J., and Friedberg, E.C. (1993). Yeast DNA repair and recombination proteins Rad1 and Rad10 constitute a single-stranded DNA endonuclease. Nature *362*, 860–862.

Tomkinson, A.E., Bardwell, A.J., Tappe, N., Ramos, W., and Friedberg, E.C. (1994). Purification of Rad1 protein from *Saccharomyces cerevisiae* and further characterization of the Rad1–Rad10 endonuclease complex. Biochemistry *33*, 5305–5311.

Troelstra, C., Landsvater, R.M., Wiegant, J., van der Ploeg, M., Viel, G., Buys, C.H.C.M., and Hoeijmakers, J.H.J. (1992). Localization of the nucleotide excision repair gene *ERCC6* to human chromosome 10q11-q21. Genomics *12*, 745–749.

van Duin, M., de Wit, J., Odjik, H., Westerveld, A., Yasui, A., Koken, M.H.M., Hoeijmakers, J.H.J., and Bootsma, D. (1986). Molecular characterization of the human excision-repair gene *ERCC-1*: homology with the yeast *RAD10* gene. Cell *44*, 913–923.

van Duin, M., Vredeveldt, G., Mayne, L.V., Odijk, H., Vermeulen, W., Klein, B., Weeda, G., Hoeijmakers, J.H.J., Bootsma, D., and Westerveld, A. (1989). The cloned human DNA excision-repair gene *ERCC-1* fails to correct xeroderma pigmentosum complementation group A through group I. Mutat. Res. *217*, 83–92.

van Vuuren, A.J., Appeldoorn, E., Odijk, H., Yasui, A., Jaspers, N.G.J., and Hoeijmakers, J.H.J. (1993). Evidence for a repair enzyme complex involving ERCC1, ERCC4, ERCC11, and the xeroderma pigmentosum group F proteins. EMBO J. *12*, 3693–3701.

van Vuuren, A.J., Appeldoorn, E., Odijk, H., Humbert, S., Moncollin, V., Eker, A.P.M., Jaspers, N.G.J., Egly, J.-M., and Hoeijmakers, J.H.J. (1995). Partial characterization of the DNA repair protein complex, containing the ERCC1, ERCC4, ERCC11, and the XPF correcting activities. Mutat. Res. *337*, 25–39.

Vermeulen, W., Scott, R.J., Rodgers, S., Muller, H.J., Cole, J., Arlett, C.F., Kleijer, W.J., Bootsma, D., Hoeijmakers, J.H.J., and Weeda, G. (1994). Clinical heterogeneity within xeroderma pigmentosum associated with mutations in the DNA repair and transcription gene *ERCC3*. Am. J. Hum. Genet. *54*, 191–200.

Wood, R.D. (1996). DNA repair in eukaryotes. Annu. Rev. Biochem. *65*, 135–167.

Wood, R., and Burki, H.J. (1982). Repair capability and the cellular age response for killing and mutation induction after UV. Mutat. Res. *95*, 505–514.

Wood, R.D., Biggerstaff, M., and Shivji, M.K.K. (1995). Detection and measurement of nucleotide excision repair synthesis by mammalian cell extracts *in vitro*. Methods *7*, 163–175.

Yamamura, K., and Ichihashi, M. (1989). Clinical and photobiological characteristics of xeroderma pigmentosum complementation group F: a review of cases from Japan. Br. J. Derm. *121*, 471–480.

Zelle, B., Berends, F., and Lohman, P.H.M. (1980). Repair of damage by ultraviolet radiation in xeroderma pigmentosum cell strains of complementation groups E and F. Mutat. Res. *73*, 157–169.

Note Added in Proof

A human cDNA and gene that correct ERCC4-defective rodent cells have been isolated by L. H. Thompson and co-workers, and the cDNA is the same as the *XPF* cDNA reported here. The reference is: Brookman, K.W., Lamerdin, J.E., Thelen, M.P., Hwang, M., Reardon, J.I., Sancar, A., Zhou, Z.Q., Walter, C.A., Parris, C.N., and Thompson, L.H. (1996). ERCC4 (XPF) encodes a human nucleotide excision repair protein with eukaryotic recombination homologs. Mol. Cell Biol., in press.